Elsevier Editorial System(tm) for
Atmospheric Environment

Manuscript Draft

Manuscript Number: ATMENV-D-18-01045R1

Title: Radon-based estimates of equivalent mixing layer heights: A long-term assessment

Article Type: Research Paper

Keywords: Radon decay products; radioactive tracer; mixing layer height; box model

Corresponding Author: Professor Roberta Vecchi, dr

Corresponding Author's Institution: Università degli Studi di Milano

First Author: Roberta Vecchi, dr

Order of Authors: Roberta Vecchi, dr; Francesco Ariele Piziali; Gianluigi Valli; Maurizio Favaron; Vera Bernardoni

Abstract: Air pollution events at urban locations are driven by both emissions and atmospheric dispersion conditions. Atmospheric dispersion is not routinely assessed at monitoring networks thus preventing the possibility of understanding if high pollution events are due to increasing emissions or to the occurrence of atmospheric stability conditions. In principle, this piece of information would be very useful to implement effective strategies for pollution abatement. In this work, an 18-year long dataset of radon (222Rn) progeny measurements was used to estimate equivalent mixing layer heights (hereafter referred to as MH) with hourly resolution by means of a box model. Mean MH obtained by more conventional modelling approaches based on turbulence variables on a 5-year long dataset agreed very well with results obtained by the box model. It is noteworthy that in the literature there are scarce MH data for such long periods and comparison between estimates by a radioactive tracers and other approaches are often limited to a few days/weeks. Results suggested that relatively simple methods like the one here proposed could be implemented at pollution monitoring stations in order to improve available information and better understand the evolution of pollution events on 1-hour timescale. In addition, the long-term assessment here presented provides useful data to pursue MH climatological studies.

Research Data Related to this Submission

There are no linked research data sets for this submission. The following reason is given:
Data will be made available on request

Radon-based estimates of equivalent mixing layer heights: A long-term assessment

Vecchi R. [1,2,*], Piziali F.A.[1], Valli G. [1,2], Favaron M. [1,3], Bernardoni V. [1,2]

[1] Department of Physics, Università degli Studi di Milano, 20133 Milan, Italy
[2] National Institute of Nuclear Physics, INFN-Milan, 20133 Milan, Italy
[3]Servizi Territorio srl, 20092 Cinisello Balsamo, Italy

[*]corresponding author: Prof. Roberta Vecchi
E-mail: roberta.vecchi@unimi.it
Address: Department of Physics, Università degli Studi di Milano, via Celoria 16, 20133 Milan (Italy)

Keywords: Radon decay products; radioactive tracer; equivalent mixing layer height; box model

Abstract

Air pollution events at urban locations are driven by both emissions and atmospheric dispersion conditions. Atmospheric dispersion is not routinely assessed at monitoring networks thus preventing the possibility of understanding if high pollution events are due to increasing emissions or to the occurrence of atmospheric stability conditions. In principle, this piece of information would be very useful to implement effective strategies for pollution abatement. In this work, an 18-year long dataset of radon (^{222}Rn) progeny measurements was used to estimate equivalent mixing layer heights (hereafter referred to as MH) with hourly resolution by means of a box model. Mean MH obtained by more conventional modelling approaches based on turbulence variables on a 5-year long dataset agreed very well with results obtained by the box model. It is noteworthy that in the literature there are scarce MH data for such long periods and comparison between estimates by a radioactive tracers and other approaches are often limited to a few days/weeks. Results suggested that relatively simple methods like the one here proposed could be implemented at pollution monitoring stations in order to improve available information and better understand the evolution of pollution events on 1-hour timescale. In addition, the long-term assessment here presented provides useful data to pursue MH climatological studies.

1. Introduction

The interpretation of air pollution events, e.g. at urban sites, relies on the knowledge of pollutants concentration, emission sources, and atmospheric dispersion conditions in the planetary boundary layer. According to e.g. Stull (1988), the planetary boundary layer (PBL) is the portion of the troposphere that is influenced by the Earth's surface forcing and responds to forcings with approximately 1-h timescale. It has a typical thickness ranging from hundreds of metres to few kilometres. With high pressure atmospheric conditions, at continental locations PBL has a well-defined structure with a daily cycle. It is composed of three main structures called mixed layer (ML, also referred to as convective layer CL), residual layer (RL), and stable layer (SL, also referred to as nocturnal boundary layer NBL). During daytime, pollutants emitted by ground-level sources are vertically dispersed in the PBL usually by convective turbulence and a well-mixed layer is produced. After sunset, convective turbulence decays and the residual layer is formed; RL has the same initial mean state variables and concentration levels of the decayed ML. During nighttime, in the lower portion of the PBL a stable layer is formed and pollutants emitted in the SL are poorly dispersed along the vertical profile. Therefore, in an ideal situation characterised by constant emissions at ground level, PBL thickness strongly determines the concentration of primary pollutants in air, i.e. higher/lower mixing height would be responsible for lower/higher pollutant concentrations.

The evaluation of atmospheric mixing height is traditionally performed through vertical profiling and/or ground-based remote sensing profile measurements (e.g. radio-soundings, sodar, lidar, radio-acoustic soundings as reviewed e.g. in Seibert et al. (2000) and Emeis et al. (2008)) as well as by numerical models (e.g. Carson, 1973; Maul, 1980; Venkatram, 1980a, 1980b; Zilitinkevich and Baklanov, 2002; Batchvarova and Gryning 1991, 1994; and many others). Profile measurements provide valuable datasets at specific locations (e.g. radio-soundings at airports or lidar measurements at EARLINET network sites); however, it is still challenging to retrieve mixing height in an automated way thus preventing the acquisition of high-time resolved datasets over long periods (e.g. 1-h, every day for decades) at the monitoring stations where pollutants are routinely measured. Simple parametrisation methods based on surface meteorological variables and numerical models are widely used by meteorological services; nevertheless, the latter are typically more sophisticated approaches and require a specific expertise. An overview of advantages and shortcomings of the above-cited methods can be found in Seibert et al. (2000).

In addition, previous works (e.g. Allegrini et al., 1994; Marcazzan and Persico, 1997; Marcazzan et al., 2003; Sesana et al., 2003; Desideri et al., 2006; Griffiths et al., 2013; Chambers et al., 2015a, b; Salzano et al., 2016) proved that measurements of natural radionuclides (such as ^{222}Rn, hereafter

69 also referred to as radon) were effective in tracing the hourly evolution of atmospheric dispersion in
70 the boundary layer. Radon and lidar or sodar measurements were also combined to retrieve MH as
71 reported in the literature (e.g. Griffiths et al., 2013; Salzano et al., 2016) for short periods
72 (days/weeks).
73 ^{222}Rn is a natural radioactive gas belonging to the natural radioactive series of ^{238}U which is a trace
74 constituent of soil and rocks. Radon is the decay product of ^{226}Ra and it is the only gaseous
75 component of the ^{238}U decay series; therefore, it is exhaled from the ground and diluted in
76 atmosphere by turbulent mixing (Porstendörfer, 1994). Radon decays (half-life $T_{1/2}$=3.82 days) into
77 daughter radionuclides, which rapidly attach to atmospheric particles due to their electric charge
78 (Porstendörfer and Mercer, 1979; Porstendörfer, 1994). Higher ^{222}Rn concentrations are typically
79 observed during stable atmospheric conditions (e.g. during nighttime) and lower concentration
80 values are measured with well-developed mixing layers (e.g. in the afternoon), as far as radon
81 exhalation flux from the ground can be considered approximately constant.
82 Seasonal patterns of radon and its decay products were observed at our monitoring site (Milan,
83 Italy) in previous studies (Marcazzan et al., 2003; Sesana et al., 2003). Typically, higher
84 concentrations were generally measured in winter in relation to more stable atmospheric conditions
85 and lower ones were detected in spring-summer, when atmospheric dilution power is more
86 effective. These features of radon concentrations motivated the use of ^{222}Rn and its progeny as a
87 suitable – although very simple – index for atmospheric dispersion.
88 From measurements of radioactive activity of atmospheric particles, a quantitative estimate of the
89 equivalent mixing height (MH) can be performed by a simple box model approach as reported in
90 previous literature works after Fontan et al. (1979) (e.g. Marcazzan and Persico, 1997; Sesana et al.,
91 2003; Griffiths et al., 2013; Chambers et al., 2015a, b; Salzano et al., 2016; and references therein).
92 A box model is also described and implemented in this work; it is noteworthy that it is applied to an
93 18-year long dataset thus allowing the robust assessment of inter-annual, seasonal, and mean daily
94 patterns. In addition, MH estimates retrieved by box model are here compared to results obtained by
95 other methodologies (i.e. parametrisation from a combination of Gryning–Batcharova and
96 Zilitinkevich modelling approaches using atmospheric turbulence variables as input data) on a 5-
97 year long subset. MH estimates by the box model are in good agreement with more traditional
98 approaches, which are not always easily implemented in monitoring networks. To the authors'
99 knowledge, this is the first time that the assessment of equivalent mixing layer height is performed
100 with hourly resolution over such a long period.
101 Despite the increasing number of pollution monitoring networks and the variety of parameters
102 measured, a simple method to routinely retrieve equivalent mixing layer heights estimates with

high-time resolution is still lacking. Therefore, this work aims at showing that box model based on radon data could give useful information on MH climatology as well as on mean daily MH evolution with hourly resolution.

2 Methods

2.1 Monitoring site

Short-lived radon decay products are routinely monitored at the Department of Physics, University of Milan (Italy). Milan (45° 28' 36" N; 9° 13' 55" E) is located in the Po valley, a well-known European pollution hot-spot characterised by wintertime episodes with high pollutant concentrations. Emissions by a variety of sources (e.g. traffic, residential heating, industries, agricultural and manure activities) and prolonged atmospheric stability conditions are responsible for high pollution levels registered (see e.g. Vecchi et al., 2007; 2009; 2018). Wind speed lower than 2 m s^{-1} are typically registered in Milan in more than 80% of the days in a year and the shelter offered by the mountain chains of the Alps and the Apennines very frequently prevent air masses replacement in the Po valley.

2.2 Radon concentration measurements

Radon short-lived decay products (^{214}Po and ^{218}Po) attached to aerosol particles are measured with 30-min resolution (and then averaged on 1-hour) by on-line alpha particle spectrometry. In the alpha spectrum, a major contribution (see Figure S1 in the Supplemental material) is given by ^{214}Po (E_α=7.685 MeV; $T_{1/2}$=163.6 μs). Due to its very short half-life, as a matter of fact ^{214}Po emission can be directly related to the emission of its precursor ^{214}Bi (β-emitter, $T_{1/2}$=19.9 min). It is noteworthy that all radon daughters are assumed to be in radioactive equilibrium and show a nearly constant disequilibrium factor with ^{222}Rn in atmosphere (exceptions are observed when unusual meteorological conditions such as heavy rainfall, frozen soil, and strong winds occur). Therefore, knowing the disequilibrium factor (at our monitoring site it was estimated in the past via parallel activity measurements of radon and its short-lived decay products), the activity concentration of ^{222}Rn can be assessed by measuring its short-lived daughters. In this work, a measured disequilibrium factor of 0.77 between short-lived decay products and radon was used to obtain ^{222}Rn concentrations (Marcazzan et al., 2003).

Only a brief description of the experimental setup will be given in the following (for further details see Marcazzan et al. (2003)). On-line alpha spectrometry is performed on atmospheric aerosols collected on a glass-fibre filter (Whatman GF/A 50 mm diameter) using a pump with sampling flowrate of 10 l/min. The sampling inlet is placed at a height of 6 metres a.g.l. and equipped with a

cyclone. The cyclone selects particles with aerodynamic diameter less than 3.5 μm in order to avoid filter clogging. As radon decay products attach preferentially to small-sized particles, this cut-off allows retaining any relevant information. Indeed, Porstendörfer et al. (2000) reported outdoor relative activity size distributions for short-lived ^{222}Rn decay products and showed that most of the activity (approximately 60%) was found on average in the accumulation mode (aerodynamic mean diameter ~ 310 nm) and less than 2% (range: 0-10%) was associated to atmospheric particles in the coarse mode (i.e. particles with aerodynamic mean diameter larger than 3 μm). To further avoid filter clogging, filter replacement is carried out weekly.

During aerosol sampling, alpha particles emitted by radon progeny collected on a filter are detected by an ion implanted silicon surface barrier detector placed in front of the filter. Each alpha spectrum is acquired for 1800 seconds and spectra acquisition is carried out repeatedly. To quantify radon progeny concentration, the first step is to subtract the contribution due to ^{220}Rn (also called thoron) progeny to the spectrum. Afterwards, ^{214}Po concentration is calculated for each spectrum making some assumptions, as shortly reported below:

1) the first hours of the sampling are corrected due to the non-equilibrium between sampled nuclides and nuclides removed by radioactive decay. This correction is needed only for the first 3 hours after the filter change;

2) counts in the alpha spectrum are assumed to be given by two contributions: the nuclides previously collected on filter and those sampled during the running measurement. The first contribution can be calculated using the result from the previous measurement because the amount of the nuclides lasting on the filter is in a given ratio with concentration calculated in the previous cycle;

3) ^{214}Pb concentration is then calculated for the i-th time interval starting from the difference between i-th and (i-1)-th (corrected as explained before) measured counts.

Minimum detection limit of this technique is 0.2 Bq m^{-3} and the overall mean uncertainty – mainly ascribed to counting statistics, uncertainty in counting efficiency, and flowrate - is typically 10% (up to 15% when approaching minimum detection limit).

Hourly radon concentrations were recorded continuously by our research group at the same monitoring site and with the same experimental methodology from 1999 to 2016 (18 years). This dataset was used as input to our box model and comprised 152692 valid hourly entries with a very small percentage of missing data (3.2%). Statistical analysis and data elaboration presented in this paper were performed using the free software environment R (R-core team, 2012) and openair package (Carslaw and Ropkins, 2012; Carslaw, 2013).

3 Radon-based mixing height modelling

3.1 Radon as a tracer for atmospheric dispersion

As mentioned before, radon is a radioactive noble gas that is emitted from the ground at a rate slowly varying in space and time (Porstendörfer, 1994). A detailed analysis on geographical patterns of radon exhalation rate is reported in the literature (e.g. Szegvary at al., 2009; IAEA, 2012; López-Coto et al., 2013). It is noteworthy that radon half-life ($T_{1/2}$= 3.82 days) is suitable for the time scale of the atmospheric processes to be investigated here. Its physical features make radon a suitable natural tracer of mixing conditions in the lower atmosphere as variations of radon activity concentration due to changes in the exhalation rate from soil are less relevant than those caused by atmospheric mixing. These variations become non-negligible only when extreme weather conditions such as heavy rain, snow, and frozen soil occur (Duenas and Fernandez, 1987; Porstendörfer, 1994).

As a result, radon concentration measurements show a typical daily pattern (Figure 1) represented by maximum concentration in early morning (5:00-7:00 LT) - after nocturnal accumulation - and minimum concentration during afternoon (16:00-18:00 LT) - when mixing layer is well-developed and vertical dispersion occurs. This typical daily pattern - also known as radon wave – suggests that it can be represented by two principal harmonic terms with periods of 24h and 12h as described in the next section (Garzon et al., 1986).

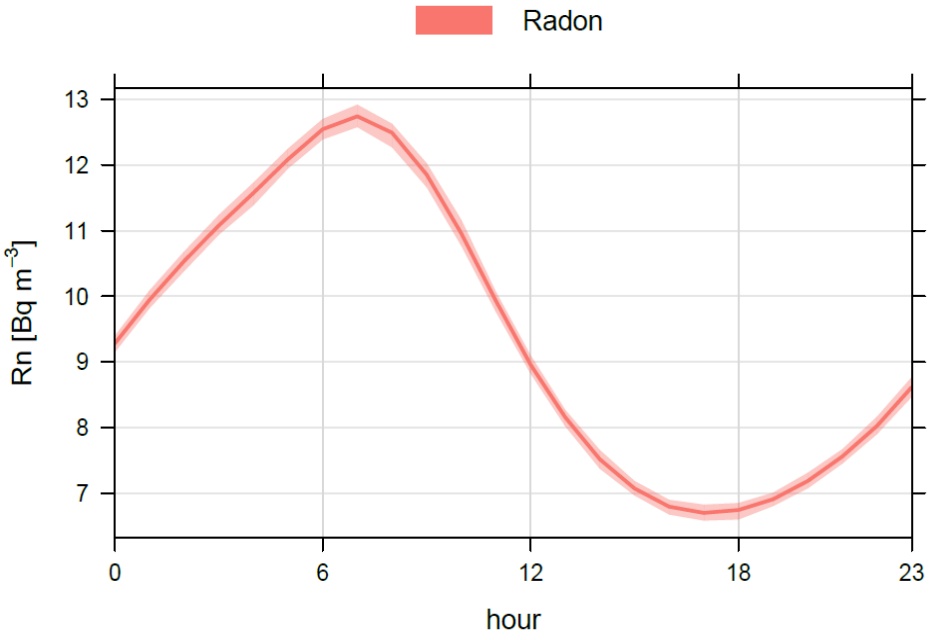

Figure 1

193 Basic statistics of ^{222}Rn concentration activity hourly values for the whole dataset (1999-2016) is
194 reported in Table 1; the average value over 18 years is 9.4 Bq m^{-3}, which is within the 9-10 Bq m^{-3}
195 range given as global average for atmospheric radon concentrations (UNSCEAR, 2000).

Valid data	152692
Overall missing data (percentage)	5108 (3.2%)
Average activity concentration (Bq m^{-3})	9.4
Median activity concentration (Bq m^{-3})	7.5
Minimum activity concentration (Bq m^{-3})	0.3
Maximum activity concentration (Bq m^{-3})	49.5

196 Table 1
197
198 **3.2 Dataset preparation**
199 Radon activity concentration measurements determined as reported in section 2.2 can be used as
200 input data for the box model here implemented.
201 No specific data pre-treatment (e.g. selective data exclusion) was adopted for the long-term analysis
202 here presented. Nevertheless, as measurements are based on the detection of alpha particle
203 emissions, they are affected by counting statistics errors which cause small statistical fluctuations in
204 the time series. The box model is very sensitive to this kind of fluctuations; indeed, the presence of
205 an increasing concentration value in a decreasing trend can determine a non-physical discontinuity
206 in the series of computed mixing heights. Therefore, a smoothing technique was applied to the time
207 series to avoid this drawback. In the smoothing procedure radon concentration data were treated
208 like a periodic signal characterised by a fundamental 24-hour component and a Fourier analysis
209 (Figure 2) of the time series was carried out to remove noise from the signal. Following the daily
210 pattern of radon concentrations shown in Figure 1, harmonics characterised by a period lower than
211 12h were rejected. This smoothing approach allowed to remove discontinuities in the temporal
212 trend, but it did not affect significantly the linear correlation between measured and smoothed
213 concentrations compared to less aggressive approaches (e.g. rejection of harmonics lower than 6h).
214 The agreement between smoothed and measured radon concentration was within 3% (Figure 3). A
215 good agreement in temporal patterns was also found as shown in the short-term pattern reported as
216 an example in Figure S2 (Supplemental material), where the smoothing temporal patterns with 6h-
217 and 12h-rejected harmonics are reported together with measured radon concentrations. It can be
218 noticed that the aggressive smoothing process affects only slightly the highest ^{222}Rn values, which
219 are sometimes a bit lower than measured concentrations.

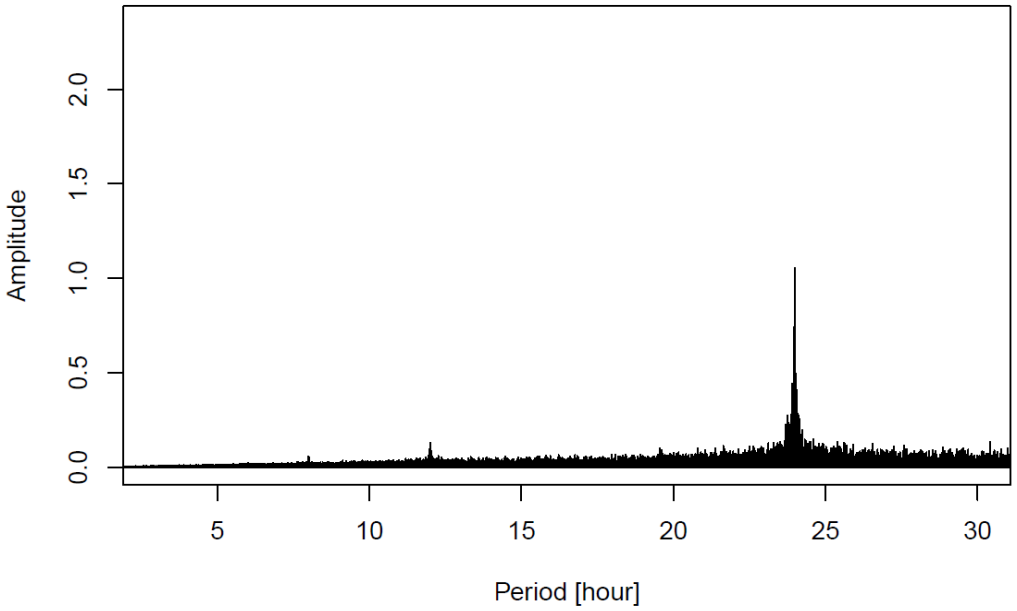

220

221 Figure 2

222

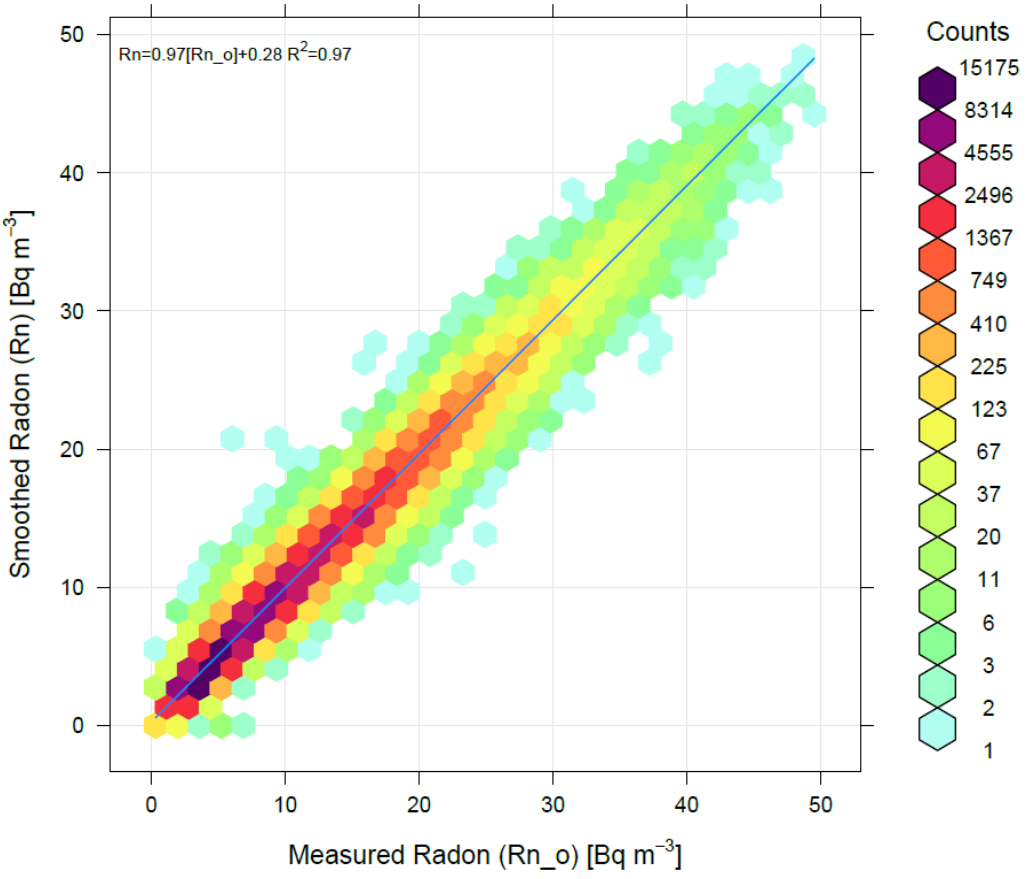

223

224 Figure 3

225

3.3 Box model implementation

In this work, equivalent mixing layer height was quantitatively assessed with hourly resolution from atmospheric radon concentrations measured at ground level using a box model. The model here applied is based on the one proposed by Marcazzan and Persico (1997) and Sesana et al. (2003), who improved the original box model (Fontan et al., 1979) taking into account the radon contribution from the atmospheric residual layer as also recently reported by other authors (e.g. Griffiths et al., 2013; Salzano et al., 2016). Indeed, RL is formed from late afternoon when MH starts to the decrease. Radon concentration existing at the time when RL forms is removed only be decay. Due to its half-time, ^{222}Rn can persist in RL till the day after and it has to be accounted for when MH increases thus progressively including air from RL.

In addition to local stability conditions, Chambers et al. (2015b) highlighted that near-surface radon concentrations can be also affected by large-scale advection phenomena and suggested to separate these two signals before using radon as a tracer for PBL stability. Rossa et al. (2012) showed that very frequent (60-80%) stagnant conditions (with Bulk Richardson Number BRN > 1) characterise the Po valley climatology and surface inversions in temperature profiles frequently occur. Therefore, at least at our monitoring site, the very poor air replacement typical of the Po valley reinforces the validity of the hypotheses made in the box model.

The modelling based on radon concentration describes both the diurnal convective layer and the nocturnal stable layer as a box, having the soil as its base and MH as its height.

By a mass balance, the equivalent mixing height can be derived under the following assumptions:

1. radon flux from the ground, i.e. radon exhalation rate, is constant;
2. atmospheric radon concentration is not affected by advection;
3. the box is vertically well-mixed;
4. radon is removed from the box only by radioactive decay;
5. a residual radon concentration is retained in the nocturnal residual layer.

In the computation a value of 0.02 Bq m^{-2} s^{-1} (i.e. the experimental value reported by Marcazzan and Persico, 1997) was used for the radon exhalation rate at the monitoring site. It is noteworthy that this value is fairly similar to the one reported in UNSCEAR (2000) as a global mean.

The procedure used to compute the equivalent mixing height is briefly outlined in the following. At every time t_i(s), knowing the radon activity concentration C_i (Bq m^{-3}) measured at ground level, the corresponding equivalent mixing height h_i in metres can be evaluated. The model is initialised in the late afternoon, when radon concentrations - after daily minimum corresponding to maximum mixing heights - start to increase (see Figure 1).

Radon mass balance is differently implemented for increasing and decreasing h_i. In fact, the variation in radon concentration within the box is governed by a balance between a surface-emission term and the radioactive decay; only in case of a growing layer also the entrainment of a residual concentration term is taken into account.

Following the typical daily temporal evolution of ML (a detailed description of ML features can be found e.g. in Stull, 1988) some assumptions are made (refer to Figure 4, where data from a typical cycle based on a real measurement performed on Sept., 27-28, 2011 are reported as an example):

1) The residual layer starts to form just after the MH reaches its maximum daily value (h_{max}, e.g. H_1=440 m in Figure 4) i.e. when the minimum radon concentration (C_{min}) is registered (at t_{min}, e,g. at 17:00 in Figure 4). Radon concentration in RL (C_R^*) remains constant to the value measured at t_{min} except for the time dependent reduction due to radioactive decay ($C_R^* = C_{min} \cdot (\exp(-\lambda(t - t_{min}))$. In the layer above RL (light lilac in Figure 4) the radon concentration is supposed to be zero.

2) When MH decreases, the two atmospheric layers (ML and RL) are decoupled and the concentration in the box is governed by a balance (see equation 1a) between a surface-emission term and radioactive decay (referring to Figure 4 this happens until 01:00 when a minimum height H_9=35 m is reached). MH is calculated by equation 1b.

3) When MH starts to increase, RL is progressively incorporated in the box and a further term accounting for RL radon concentration adds to the balance equation (see equation 2a). MH is calculated by equation 2b.

4) If MH exceeds the previous daily maximum ML height (referring to Figure 4 at 13:00 with H_{21}=449 m, that is higher than H_1=440m=h_{max}), the contribution due to RL concentration term is limited to the part of the box reaching the previous day maximum ML (H_{21}-H_1) as shown in equations 3a. MH is calculated by equation 3b.

5) When MH starts to decrease again, a new maximum (e.g. at 16:00 H_{24}=625 m) is taken into account in the calculation and the cycle (see point 2) restarts (H_{24} is set as H_1 for the new daily cycle).

The equations used in the above-mentioned procedure are given below:

i) for decreasing equivalent mixing height in the time interval $\Delta t = t_{i+1} - t_i$, i.e. when $h_{i+1} < h_i$,

$$h_{i+1}C_{i+1} = \frac{\Phi}{\lambda} \cdot (1 - \exp(-\lambda \Delta t)) + h_{i+1}C_i \exp(-\lambda \Delta t) \quad (1a)$$

$$h_{i+1} = \frac{\Phi}{\lambda} \cdot \frac{(1 - \exp(-\lambda \Delta t))}{C_{i+1} - C_i \exp(-\lambda \Delta t)} \quad (1b)$$

ii) for increasing equivalent mixing height in the time interval Δt, i.e. when $h_{i+1} > h_i$,

$$h_{i+1}C_{i+1} = \frac{\Phi}{\lambda}\,(1-\exp(-\lambda\Delta t)) + h_i C_i \exp(-\lambda\Delta t) + (h_{i+1} - h_i)C_R^* \quad (2a)$$

$$h_{i+1} = \frac{\frac{\Phi}{\lambda}(1-\exp(-\lambda\Delta t)) + h_i\,(C_i \exp(-\lambda\Delta t) - C_R^*)}{C_{i+1} - C_R^*} \quad (2b)$$

iii) for increasing equivalent mixing height in the time interval Δt and $h_{i+1} > h_{max}$

$$h_{i+1}C_{i+1} = \frac{\Phi}{\lambda}\left(1-\exp(-\lambda\Delta t)\right) + h_i C_i \exp(-\lambda\Delta t) + (h_{max} - h_i)\,C_R^* \quad (3a)$$

$$h_{i+1} = \frac{\frac{\Phi}{\lambda}\left(1-\exp(-\lambda\Delta t)\right) + h_i\,C_i\,\exp(-\lambda\Delta t) + (h_{max} - h_i)\,C_R^*}{C_{i+1}} \quad (3b)$$

where Φ (Bq m^{-2} s^{-1}) is the radon flux from ground; λ (s^{-1}) is the radon decay constant; C_i and C_{i+1} (Bq m^{-3}) are radon concentrations at t_i and t_{i+1}; $C_R^* = C_{min}\cdot(\exp(-\lambda(t_{i+1} - t_{min}))$ (Bq m^{-3}) is residual radon concentration at t_{i+1} computed considering the minimum concentration registered in the previous 24 hours and accounting for radioactive decay; h_{max} is the maximum MH registered during the previous day.

The presence of a single inversion layer in temperature vertical profiles registered in more than 90% of the cases analysed in a dataset (Antonioli, 2017) comprising over 30 years of radio-soundings taken at Milano-Linate airport, which is not far from our monitoring site, supported the reliability of the above-mentioned approach. It is worthy to note that all calculations assume that radon is well-mixed in the residual layer; results shown in section 4.2, seems to confirm the validity of these hypotheses.

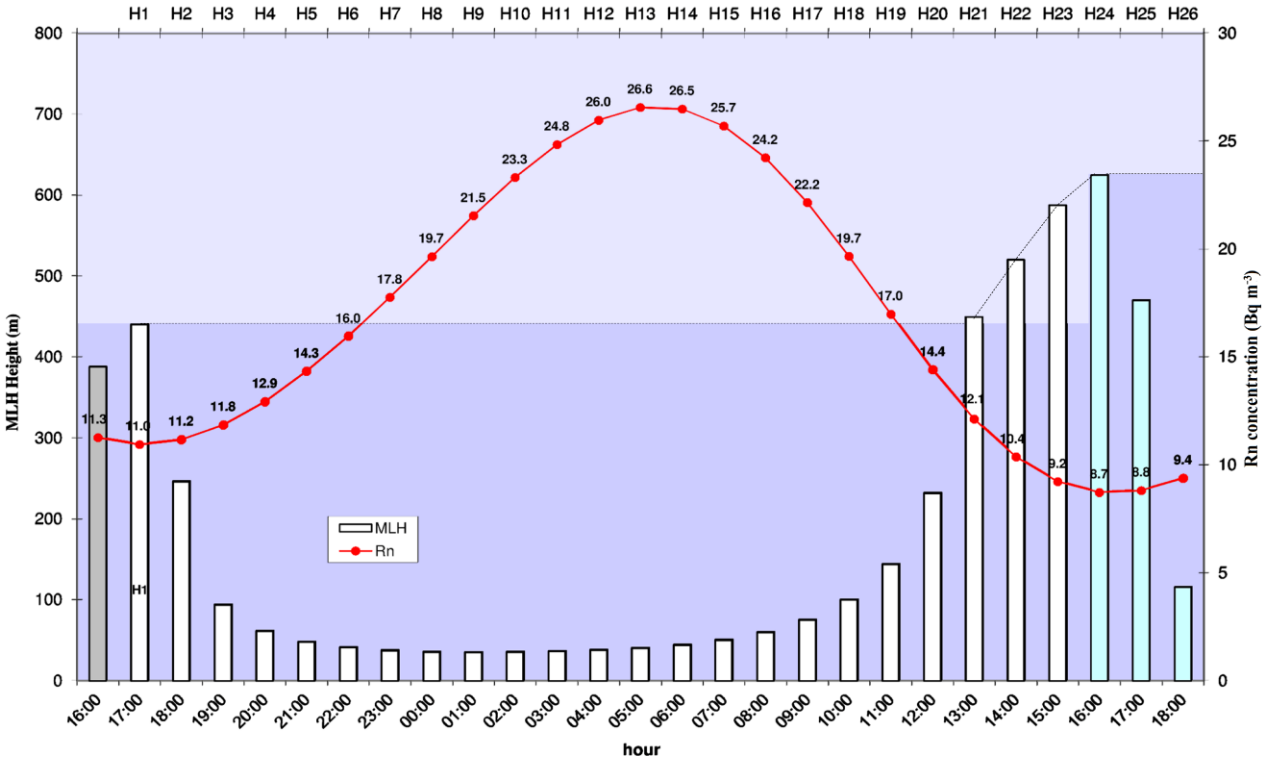

Figure 4

3.4. Equivalent mixing layer height estimates by sonic anemometer data

Equivalent mixing layer height can be estimated using both diagnostic and prognostic mathematical models, in most cases optimised for stable, near-neutral and convective conditions. The Zilitinkevich model for stable conditions (Zilitinkevich and Baklanov, 2002), the Batchvarova-Gryning model for convective conditions (Batchvarova and Gryning, 1991, 1994), and the Venkatram model (Venkatram, 1980a, 1980b) are promising MH estimation methods. For all these models, input data are turbulence parameters like Obukhov length and friction velocity, whose value is often estimated from solar radiation and temperature conventional measurements (Holtslag and van Ulden, 1982, 1983). Unfortunately, the accuracy of these estimates is difficult to assess, and direct measurement of Obukhov length and friction velocity is preferable. Direct measurement of Obukhov length and friction velocity demands use of specialised sensors like three-dimensional ultrasonic anemometers and other wind and temperature fast sensors. In our region, this task is accomplished by the regional environmental protection agency (ARPA Lombardia) through the SHAKEUP network. SHAKEUP stations are equipped with a three-dimensional ultrasonic anemometer coupled with a real-time eddy-covariance data processing system, and complemented with thermometer, hygrometer, global radiometer, rain gauge, mechanical anemometer, and barometer.

Processed data, available on request by ARPA Lombardia, include high-resolution (i.e. 10-min averages) wind data and turbulence indicators such as Obukhov length, friction velocity, and turbulent sensible heat flux.

The dataset used in this paper is from one of the nodes in the SHAKEUP network, i.e. Parco Nord, located about 10 km North of our monitoring station. It was processed by discriminating among stable, near-neutral, and convective conditions based on turbulent sensible heat flux value. In case of stable situation both Venkatram and Zilitinkevich models were applied directly, and the larger of the two estimates was retained. In convective hours, Batchvarova-Gryning model was applied assuming zero subsidence velocity above mixing layer, and temperature dry lapse rate.

4. Results

4.1 Equivalent mixing layer height estimates from radon data

MH obtained by box model were averaged on a monthly basis for daylight and nighttime separately (see Figure S3 in Supplemental Material). Daylight refers to periods between sunrise and sunset (nighttime between sunset and sunrise) considering the latitude and longitude of the measurement location as well as the day of the year. Figure S3 showed a clear seasonal trend for daylight data: the lowest MH was registered in December on average (199 m), with a minimum monthly mean of 127 m in December 2015. The highest MH was registered in May on average (556 m), with a maximum monthly mean of 688 m in May 2014. The seasonal trend is less evident for nighttime data. Nevertheless, also for these data the lowest MH was registered in December on average (184 m), with a minimum monthly mean of 124 m in December 2015. As for the highest MH in nighttime data, it was registered in May on average (312 m), with the maximum monthly mean occurring in April 2015 (446 m).

As far as long-term trend is concerned, seasonal Mann-Kendall test (Hirsch et al., 1982) was carried out on the two series: $p>0.05$ was registered in both cases, thus not enough evidence of long term monotonic trend is present in both time series.

Monthly boxplots for daylight and nighttime data are shown in Figure 5a and Figure 5b, respectively. They represent statistics (median and 5, 25, 75, 95 percentiles) referred to 1-h resolved data thus explaining the highest range of values spanned compared to Figure S3 in the Supplementary Material. It can be noticed that MH higher than 1000 m can be occasionally reached mainly during spring and summer. This representation confirms that daylight mean MH was typically higher during springtime and – although to a less extent – the same can be observed in nighttime MH. The temporal behaviour observed in springtime could be related to the atmospheric temperature lapse rate referred to ground level. As an example, Figure S4 in Supplemental Material

showed a more pronounced gradient going from winter to spring rather than from summer to autumn. This can be explained considering seasonal differences in the thermal inertia of the atmosphere and more frequent instability conditions in springtime. Indeed, relatively cold layers were still present in the upper part of the atmosphere during springtime while lower layers were heated thus fostering atmospheric vertical instability; opposite, a smooth cooling of the lower layers going from summer to autumn months produced less mixing.

MH typical daily patterns averaged over 18 years separately for each season are represented in Figure 6. It can be noticed that: (1) minima occurred in the morning between 03:00 and 07:00 with little seasonal differences being MH at most 215 m for spring minimum; (2) maxima values had a much higher variability with seasons going from about 360 m in winter up to 878 m in spring during the time slot 16:00-18:00.

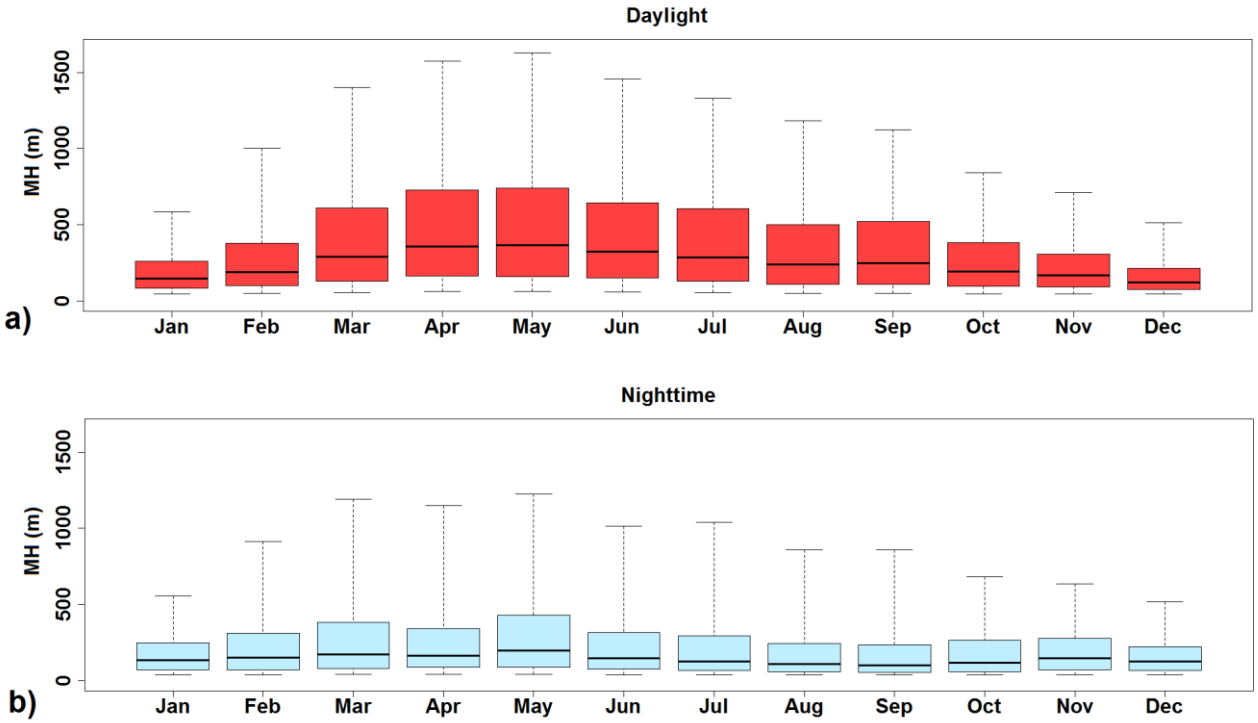

Figure 5

In Figure 6, wintertime daily pattern showed the slowest change in concentrations and the maximum appeared later than in other seasons (as a consequence, apparently winter and autumn patterns overlap during evening hours). It is not clear to the authors the reason for such delay but a stronger thermal inertia in wintertime can have played a role. Indeed, the ground was very cold during nighttime/early morning and the energy available for atmospheric convection was much less

386 in winter; therefore, heating up the atmosphere might require a longer time thus producing the delay
387 in MH peak.
388

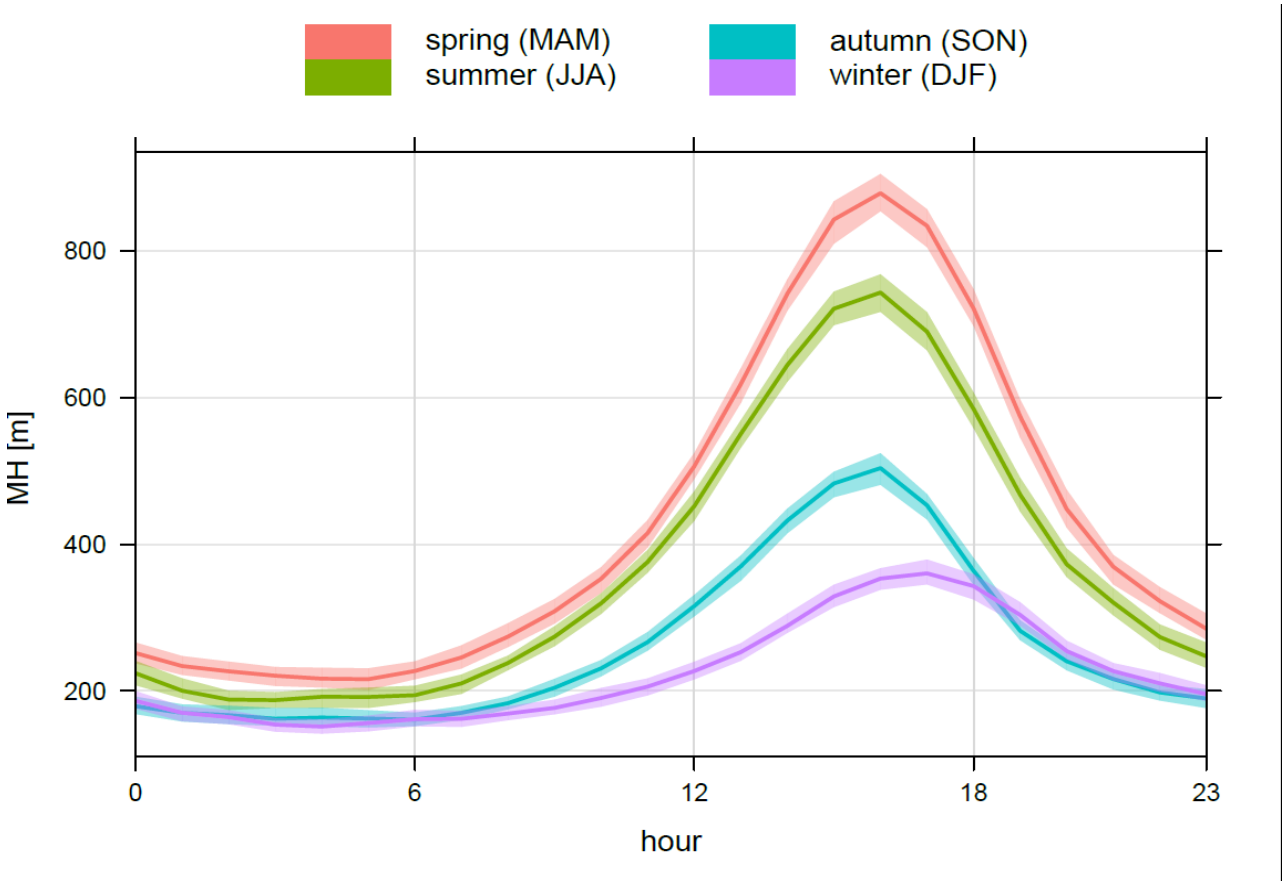

389
390 Figure 6
391
392 **4.2 Comparison between radon-based and turbulence-based equivalent mixing height**
393 **estimates**
394 The comparison between equivalent mixing layer heights estimated by radon-based (box model)
395 and turbulence-based approaches was carried out considering a data subset of five years (2012-
396 2016, i.e. on the only data available from sonic anemometer measurements).
397 In Figure 7, a comparison of MH estimates obtained by the two approaches is shown by boxplots
398 for each season. Small differences in median values can be noticed. Nevertheless, the distribution of
399 turbulence-based MH estimates seems less skewed than the radon-based one in all seasons but
400 summer. This can be partially related to the absence of data pre-selection (i.e. both models were run
401 with no pre-conditioning as a function of other variables e.g. wind speed) and to the assumption of
402 regular vertical profile of potential temperature for the turbulence-based model.

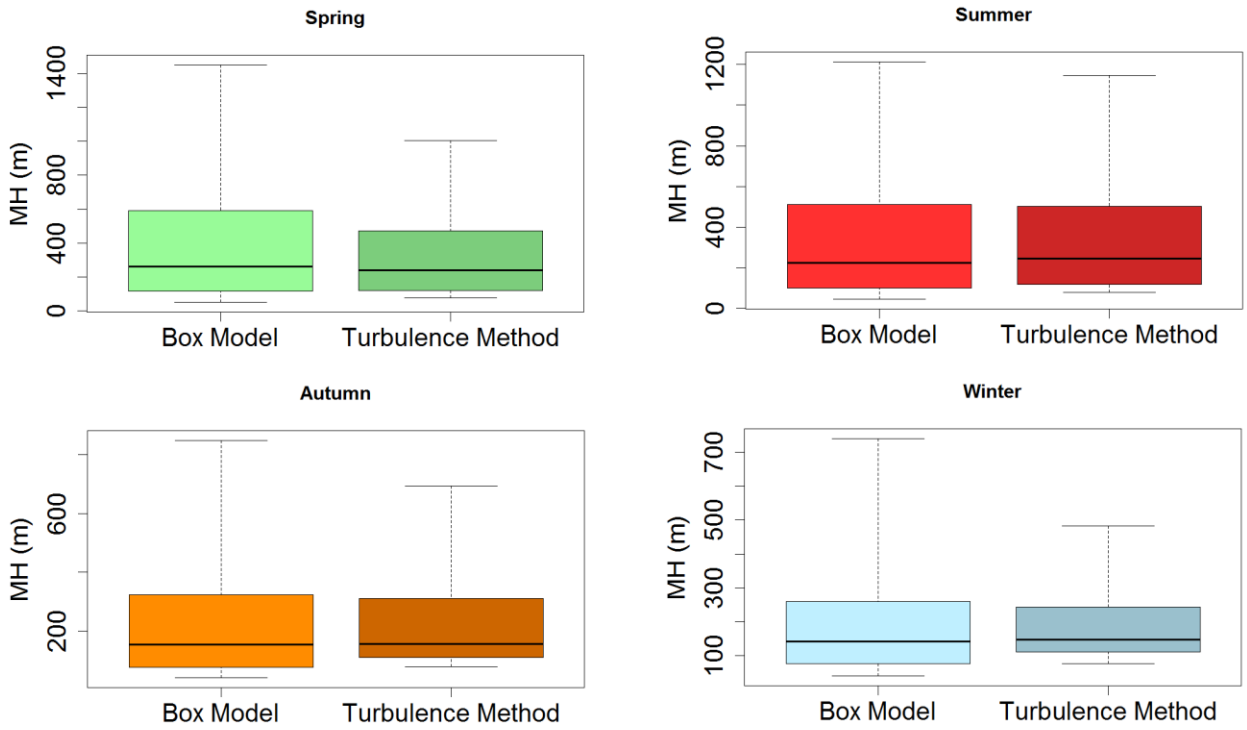

Figure 7

Figure 8 represents the scatterplot of seasonal MH mean values by radon- and turbulence-based modelling. Deming regression was applied to the data, using 1 as variance ratio between the populations. Data were fairly well correlated (R=0.89) and the Deming regression angular coefficient was 0.90 (intercept was forced to zero as resulted comparable to zero within standard error). Therefore, the agreement between the seasonal estimates by the two approaches was within 10%.

Although the main focus of this paper is on the long-term MH assessment to pursue climatological studies, it is noteworthy that both approaches estimated MH with hourly resolution (see Figure S5). Seasonal daily maximum values showed an overall agreement but for spring, when box model estimates resulted systematically higher – $p<0.05$ using a Mann-Whitney test (Mann and Whitney, 1947) – than those evaluated by the turbulence-based model. Besides the fairly good agreement in absolute values, interesting differences in hourly patterns were singled out. The box model reproduced a MH hourly pattern with a much slower decrease in the afternoon compared to quite typical fast decrease given by the turbulence-based method. MH estimated by the box model during early morning/night time were typically higher but in autumn and winter differences were much less pronounced. A certain degree of disagreement in hourly patterns is not surprising as the two methods rely on totally different parameters, i.e. the radon concentration in the box model and the

three wind components and heat flux in the other case; therefore, differences in the dynamics of the temporal evolution could be expected. A possible role might be played by characteristic times of the measurements; indeed, turbulence variables typically have very fast rate of change while the box model uses radon concentration, whose assessment is carried out on much slower times. This feature of radon measurement might yield to a MH temporal pattern which is intrinsically smoother than turbulent estimate. However, this different behaviour claims for further investigation not performed in this work and a comparison with other experimental and/or modelling approaches would be also useful.

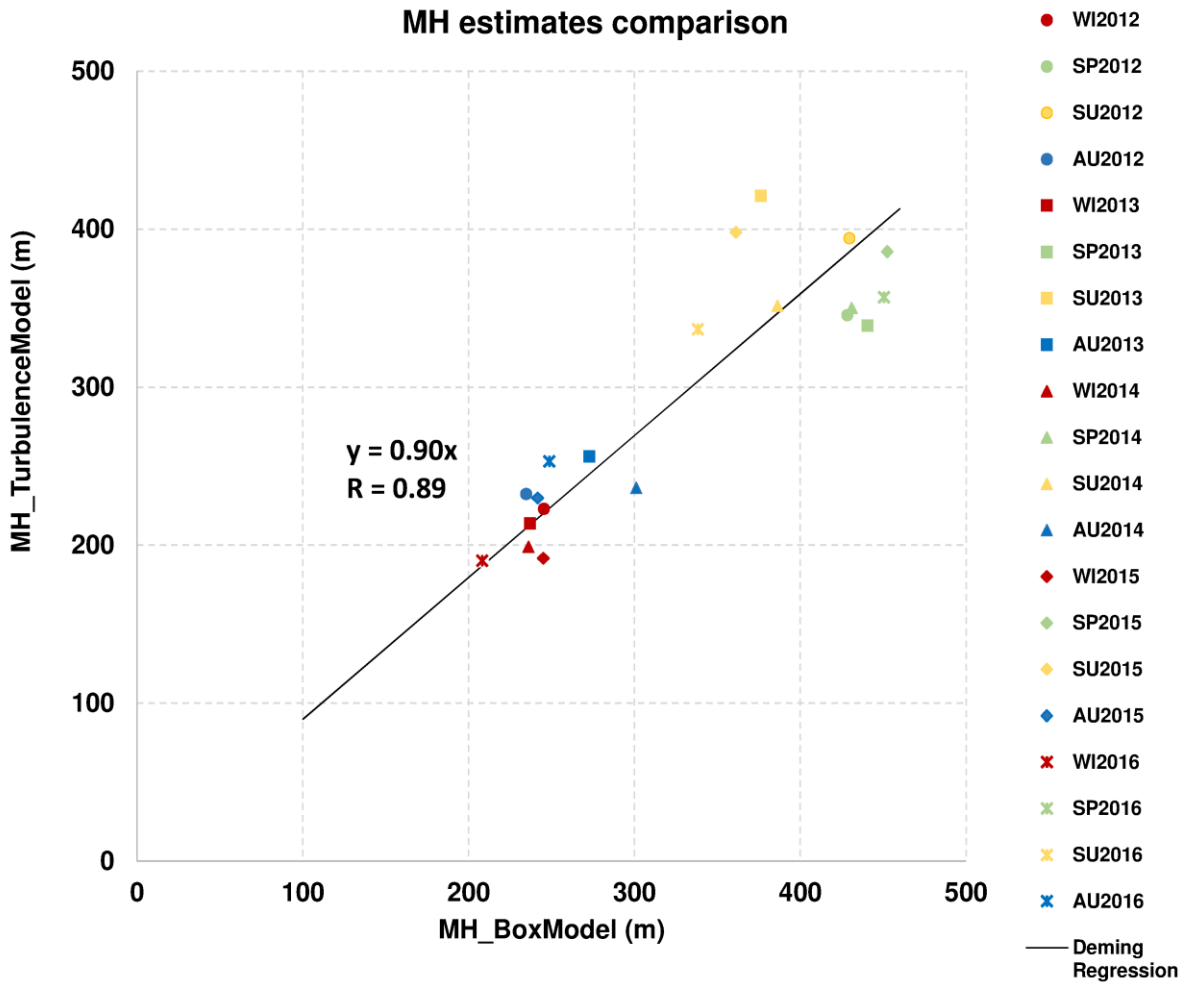

Figure 8

5. Conclusions

The assessment of equivalent mixing layer heights in Milan (Italy) over 18-years has proved that a simple box model relying on ^{222}Rn measurements can be useful for MH climatological studies. This

piece of information can be exploited in further studies to disentangle the effect of emissions from atmospheric dilution in pollution concentration data series.

Results found in this paper have shown that no relevant long-term trend affect equivalent MH in Milan (Italy) over 18 years. The availability of a statistically significant dataset evidenced seasonal differences, i.e. the highest MH were recorded typically during springtime and minima during winter months. This result suggests that springtime atmospheric instability is a driving force stronger than summertime thermals in promoting more effective air exchange on the vertical.

Using a subset of data (5-year long), MH estimates obtained by the box model were compared to those retrieved by modelling approaches using turbulence variables (obtained by sonic anemometer data) as inputs. The agreement between the seasonal averages of equivalent mixing layer height mean values estimated by two methods was very good. Furthermore, seasonal daily maxima estimates resulted comparable between the approaches (but for spring). Nevertheless, interesting differences came out when looking at daily temporal patterns. Further studies may be worth in order to understand the physical processes causing the observed differences in the MH increase/decrease features and in mean values detected in springtime.

Despite the simple box model approach here applied, results have shown that MH temporal behaviour can be estimated from radioactive tracer measurements carried out using experimental methodologies that could be effectively implemented in pollution monitoring networks adding valuable information for pollution events interpretation.

Contributors

R. Vecchi conceived and designed the study; G. Valli and V. Bernardoni performed radon measurements; G. Valli made data reduction and validation and, together with R. Vecchi, contributed to radon data interpretation; A.F. Piziali analysed long-term radon data series and, together with G. Valli, set up the box model; M. Favaron collected sonic anemometer data and run the model based on sonic anemometer data. R. Vecchi drafted the paper and all co-authors revised the manuscript content and gave a final approval of the version to be submitted.

Acknowledgements and funding

The authors thank very much ARPA Lombardia for SHAKEUP data availability and are grateful to all students who contributed to radon data collection. This research was partly funded by the Ministry of Research (COFIN2003 project) and the University of Milan (PUR2008).

References

Allegrini, I., Febo, A., Pasini, A., Schiarini, S. (1994). Monitoring of the nocturnal mixed layer by means of particulate radon progeny measurement. J Geophys Res 99(D9), 18765–18777.

Antonioli, S. (2017). Lapse rate inversions in the Po Valley: a 30-year overview. Master Thesis in Environmental and Land Planning Engineering at Politecnico di Milano, Italy. http://hdl.handle.net/10589/133660

Batchvarova, E., Gryning, S.E. (1991). Applied Model for the Growth of the Daytime Mixed Layer. Boundary Layer Meteorol 56, 261-274.

Batchvarova, E., Gryning, S.E. (1994). An Applied Model for the Height of the Daytime Mixed Layer and the Entrainment Zone. Boundary Layer Meteorol 71, 311-323.

Carslaw, D.C. and K. Ropkins, (2012). openair — an R package for air quality data analysis. Environ Model Softw 27-28, 52-61.

Carslaw, D.C. (2013). The openair manual — open-source tools for analyzing air pollution data. Manual for version 0.8-0, King's College London.

Carson, D.J. (1973). The Development of a Dry Inversion-Capped Convectively Unstable Boundary Layer. Quart J R Meteorol Soc 99, 450-467.

Chambers, S.D., Williams, A.G., Crawford, J., Griffiths, A.D. (2015a). On the use of radon for quantifying the effects of atmospheric stability on urban emissions. Atmos Chem Phys 15, 1175–1190.

Chambers, S.D., Wang, F., Williams, A.G., Xiaodong, D., Zhang, H., Lonati, G., Crawford, J., Griffiths, A.D., Ianniello, A., Allegrini, I. (2015b). Quantifying the influences of atmospheric stability on air pollution in Lanzhou, China, using a radon-based stability monitor. Atmos Environ 107, 233–243.

Desideri, D., Roselli, C., Feduzi, L., Meli, M.A. (2006). Monitoring the atmospheric stability by using radon concentration measurements: a study in a Central Italy site. J Radioanal Nucl Chem 270(3), 523–530.

Duenas, C., Fernandez, M.C. (1987). Dependence of radon 222 flux on concentrations of soil gas and air gas and an analysis of the effects produced by several atmospheric variables. Annales Geophysicae, 5B(6), 533-540.

Emeis, S., Schäfer, K., Münkel, C. (2008). Surface-based remote sensing of the mixing-layer height – a review. Meteorologische Zeitschrift 17(5), 621-630.

Fontan, J., Guedalia, D., Druilhet, A., Lopez, A. (1979). Une methode de mesure de la stabilite verticale de l'atmosphere pres du sol. Boundary Layer Meteorol 17(1), 3–14.

Garzon, L., Juanco, J.M., Perez, J.M., Fernandez, J.M., Arganza, B. (1986). The universal Rn wave. An approach. Health Phys 51(2), 185–195.

508 Griffiths, A.D., Parkers, S.D., Chambers, S.D., McCabe M.F., Williams, A.G. (2013). Improved
509 mixing height monitoring through a combination of lidar and radon measurements. Atmos Meas
510 Tech 6, 207-218.
511 Hirsch, R.M., Slack, J.R. and Smith, R.A. (1982), Techniques for trend assessment for monthly
512 water quality data, Water Resour Res 18, 107-121.
513 Holtslag, A.A.M., van Ulden, A.P. (1982). Simple estimates of night time surface fluxes from
514 routine weather data. KNMI Scientific Report. W.R. 82-4, 11pp
515 Holtslag A.A.M., A.P. van Ulden (1983). A simple scheme for daytime estimates of the surface
516 fluxes from routine weather data. J Clim and Appl Meteorol 22, 517-529.
517 IAEA, International Atomic Energy Agency (2012). Sources and measurements of radon and radon
518 progeny applied to climate and air quality studies. Proceedings Series - International Atomic Energy
519 Agency.
520 López-Coto, I, Mas, J.L., Bolivar, J.P. (2013). A 40-year retrospective European radon flux
521 inventory including climatological variability. Atmos Environ 73, 22-33.
522 Mann, H.B., Whitney, D.R. (1947). On a Test of Whether one of Two Random Variables is
523 Stochastically Larger than the Other. Ann Math Statist 18(1), 50-60.
524 Marcazzan, G.M., Persico F. (1997). Valutazione dell'altezza dello strato rimescolato a Milano
525 dall'andamento temporale della concentrazione di ^{222}Rn in atmosfera. Ingegneria Ambientale 26(7),
526 419-427. (in Italian)
527 Marcazzan, G.M., Caprioli, E., Valli, G., Vecchi, R. (2003). Temporal variation of ^{212}Pb
528 concentration in outdoor air of Milan and a comparison with^{214}Bi. J Environ Radioact 65, 77-90.
529 Maul, P.R. (1980). Atmospheric transport of sulfur compound pollutants. Central Electricity
530 Generating Bureau, MID/SSD/80/0026/R, Nottingham, England.
531 Porstendörfer, J. and Mercer, T.T., 1979; Influence of electric charge and humidity upon the
532 diffusion coefficient of radon dacay products. Health Phys 37, 191-199.
533 Porstendörfer, J. (1994). Properties and behaviour of radon and thoron and their decay products in
534 the air. J Aerosol Sci 25(2), 219–263.
535 Porstendörfer, J., Zock, C., Reineking, A. (2000). Aerosol size distribution of the radon progeny in
536 outdoor air. J Environ Radioact 51, 37-48.
537 R Core Team (2012). R: A language and environment for statistical computing. R Foundation for
538 Statistical Computing, Vienna, Austria. ISBN 3-900051-07-0, *http://www.R-project.org/*
539 Rossa, A., Ferrario, M. E., Sansone, M., and Monai, M. (2012). Climatology of the static stability of
540 the night-time Po Valley pbl from radio sondes and passive microwave radiometers. Proceedings of

the 9th International Symposium on Tropospheric Profiling, edited by Cimini, D., Di Girolamo, P., Marzano, F. S., and Rizi, V., L'Aquila, Italy ESA Conference Bureau, Noordwijk, the Netherlands.

Salzano R., Pasini A., Casasanta G., Cacciani M., Perrino C. (2016). Quantitative Interpretation of Air Radon Progeny Fluctuations in Terms of Stability Conditions in the Atmospheric Boundary Layer. Boundary Layer Meteorol 160, 529–550.

Seibert, P., Beyrich, F., Gryning, S.-E., Joffre, S., Rasmussen, A., and Tercier, P. (2000). Review and intercomparison of operational methods for the determination of the mixing height. Atmos Environ 34, 1001–1027.

Sesana, L., Caprioli, E., Marcazzan, G.M.(2003). Long period study of outdoor radon concentration in Milan and correlation between its temporal variations and dispersion properties of atmosphere. J Environ Radioact 65,147–160.

Stull R.B. (1988). An Introduction to Boundary Layer Meteorology. Kluwer Academic Publishers

Szegvary, T., Conen, F., Ciais, P. (2009). European ^{222}Rn inventory for applied atmospheric studies. Atmos Environ 43 (8), 1536–1539.

UNSCEAR, United Nations Scientific Committee on the Effects of Atomic Radiation (2000). Sources and effects of ionizing radiation. Report Volume 1.

Vecchi, R., Marcazzan, G., Valli, G. (2007). A study on nighttime-daytime PM10 concentration and elemental composition in relation to atmospheric dispersion in the urban area of Milan (Italy). Atmos Environ 41, 2136-2144.

Vecchi, R., Bernardoni, V., Fermo, P., Lucarelli, F., Mazzei, F., Nava, S., Piazzalunga, A., Prati, P., Valli, G. (2009). 4-hours resolution data to study PM10 in a "hot spot" area in Europe. Environ Monit and Assess 154, 283-300.

Vecchi, R., Bernardoni, V., Valentini, S., Piazzalunga, A., Fermo, P., Valli, G. (2018). Assessment of light extinction at a European polluted urban area during wintertime: Impact of PM1 composition and sources. Environ Poll 233, 679-689.

Venkatram A. (1980a). Estimating the Monin-Obukhov length in the stable boundary layer for dispersion calculations. Boundary Layer Meteorol 19, 481-485.

Venkatram A. (1980b). Estimation of turbulence velocity scales in the stable and unstable boundary layer for dispersion application. Eleventh NATO/CCMS International Technical Meeting on Air Pollution Modeling and its Applications, 54-56.

Zilitinkevich S., A. Baklanov (2002). Calculation of the Height of the Stable Boundary Layer in Practical Applications. Boundary Layer Meteorol 105, 389-409.

List of captions – Tables and Figures

Table 1: basic statistics on Radon activity concentrations from 1999 to 2016 (in Bq m^{-3}).

Figure 1: mean daily pattern for ^{222}Rn concentrations averaged over the period 1999-2016. A 95% confidence interval of the mean obtained by a bootstrap approach is shown.

Figure 2: Fourier spectrum of ^{222}Rn hourly concentration measured during the period 1999-2016.

Figure 3: Smoothed (Rn) vs. measured (Rn_o) radon concentrations (in Bq m^{-3}, whole dataset). The solid line is the regression line ($Rn = 0.97 \cdot Rn\_o + 0.28$; $R^2 = 0.97$).

Figure 4: Example of equivalent mixing height temporal evolution as used in the box model. Red line and dots represent Radon concentration (right axis). Bars represent MH (left axis): grey bar indicates the last MH calculated for the previous daily cycle, white bars indicate current daily cycle, light blue bars indicate the next daily cycle. Lilac area represents mixing+residual layer (ML+RL) whereas light lilac area represents the layer above the RL.

Figure 5: boxplot of MH monthly statistics for daylight (a) and nighttime (b). The horizontal line represents the median, the coloured box is 25-75th percentile range and the whiskers extend between 5-95th percentiles. Daylight refers to periods between sunrise and sunset (nighttime between sunset and sunrise) considering the latitude and longitude of the measurement location as well as the day of the year.

Figure 6: Typical daily pattern of the equivalent mixing layer height in different seasons averaged over the period 1999-2016. A 95% confidence interval for the mean value evaluated by bootstrap is shown.

Figure 7: Comparison between MH estimated by the radon- and turbulence-based models. The horizontal line represents the median, the coloured box is 25-75th percentile range and the whiskers extend between 5-95th percentiles.

Figure 8: Scatterplot of seasonal averages of MH estimates obtained by radon-based box model and turbulence model in different years. Regression line refers to Deming regression. The different markers represent seasons (colours) and years (shape). Legend interpretation: Spring (SP)=March-

May, Summer (SU)=June-August, Autumn (AU)=September-November, Winter (WI)=December-February. As for winter, the year in the legend refers to January and February.

Figure 1

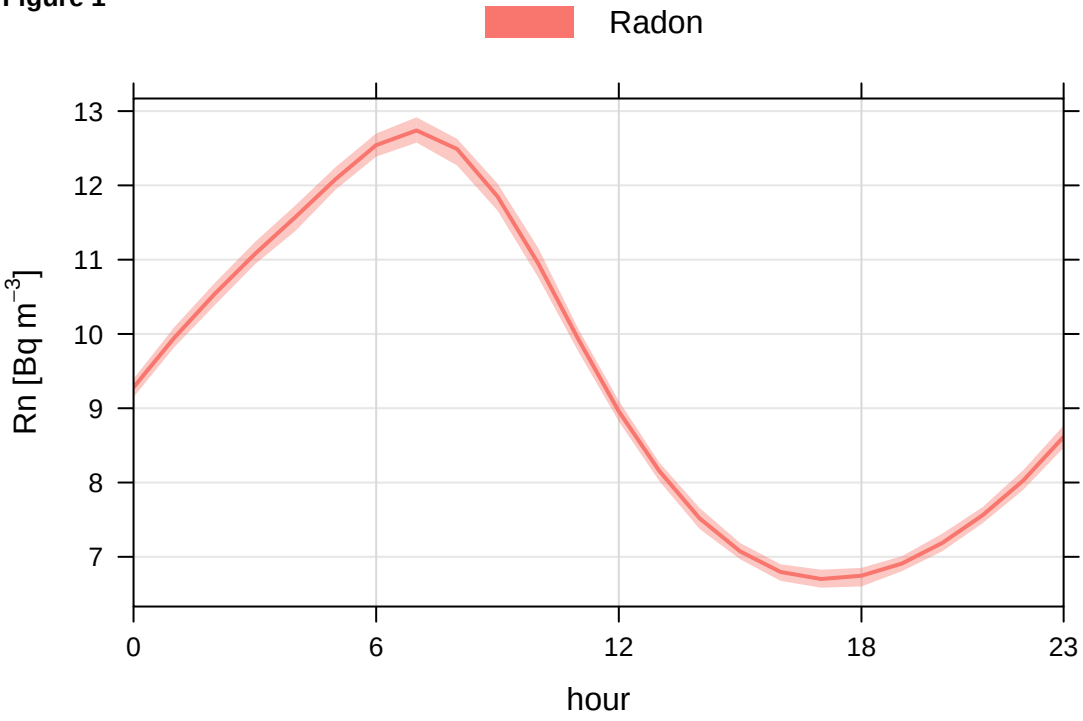

Figure 2

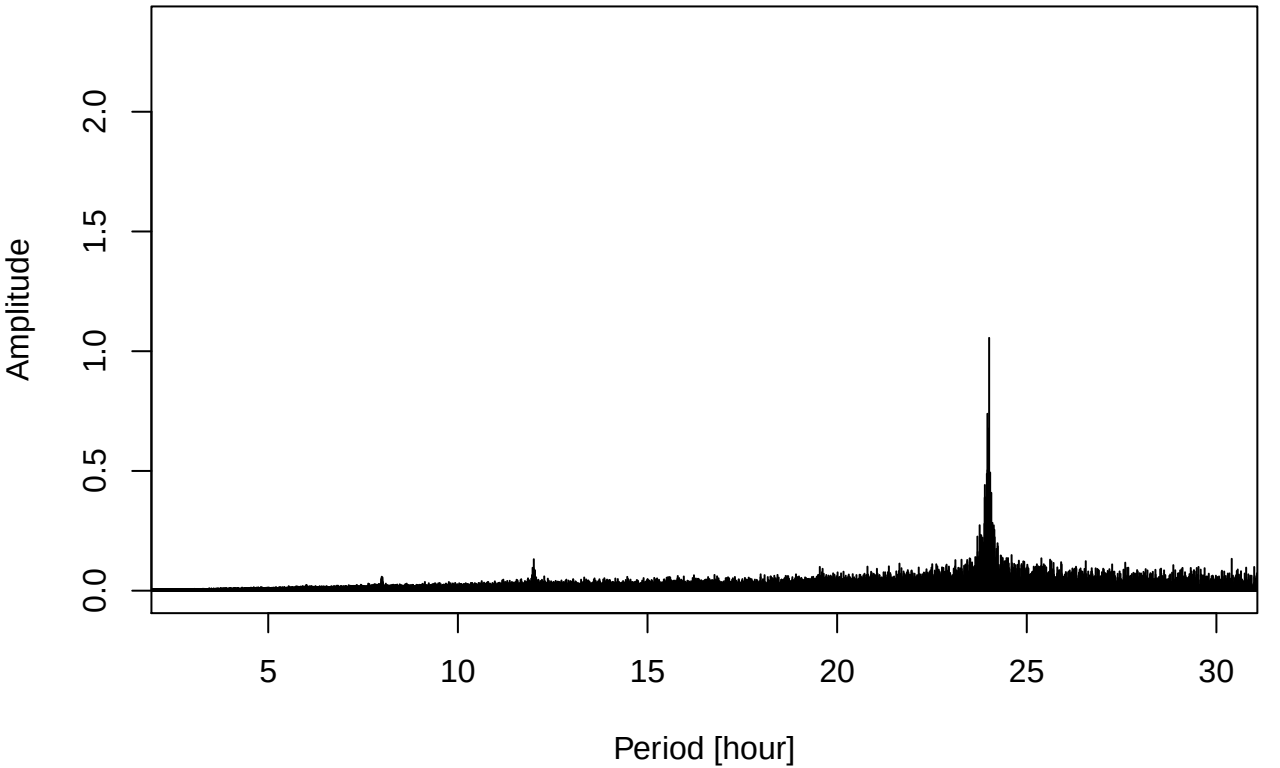

Figure 3

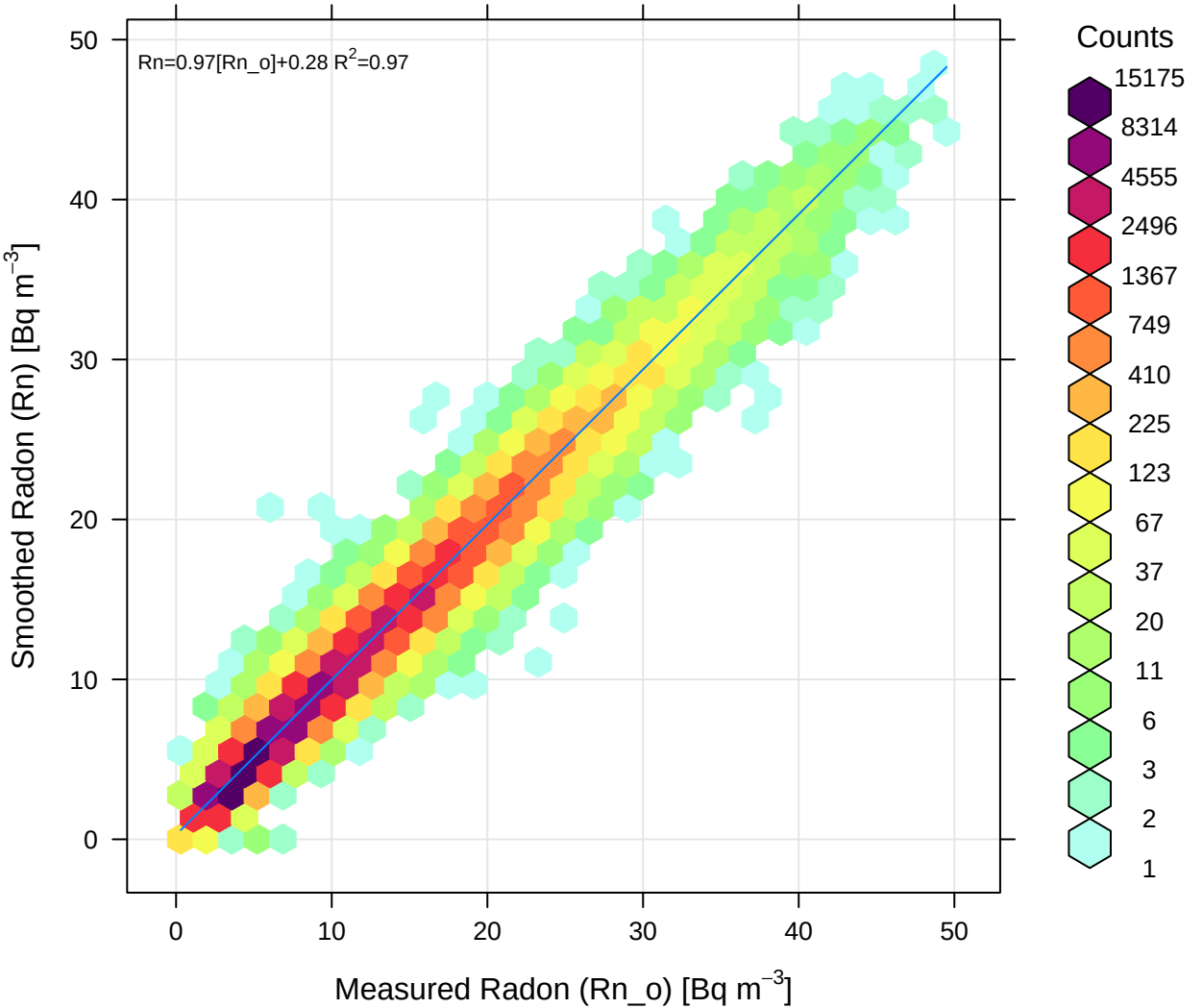
Rn=0.97[Rn_o]+0.28 R2=0.97
Smoothed Radon (Rn) [Bq m−3]
Measured Radon (Rn_o) [Bq m−3]
0
10
20
30
40
50
Counts
15175
8314
4555
2496
1367
749
410
225
123
67
37
20
11
6
3
2
1

Figure 4

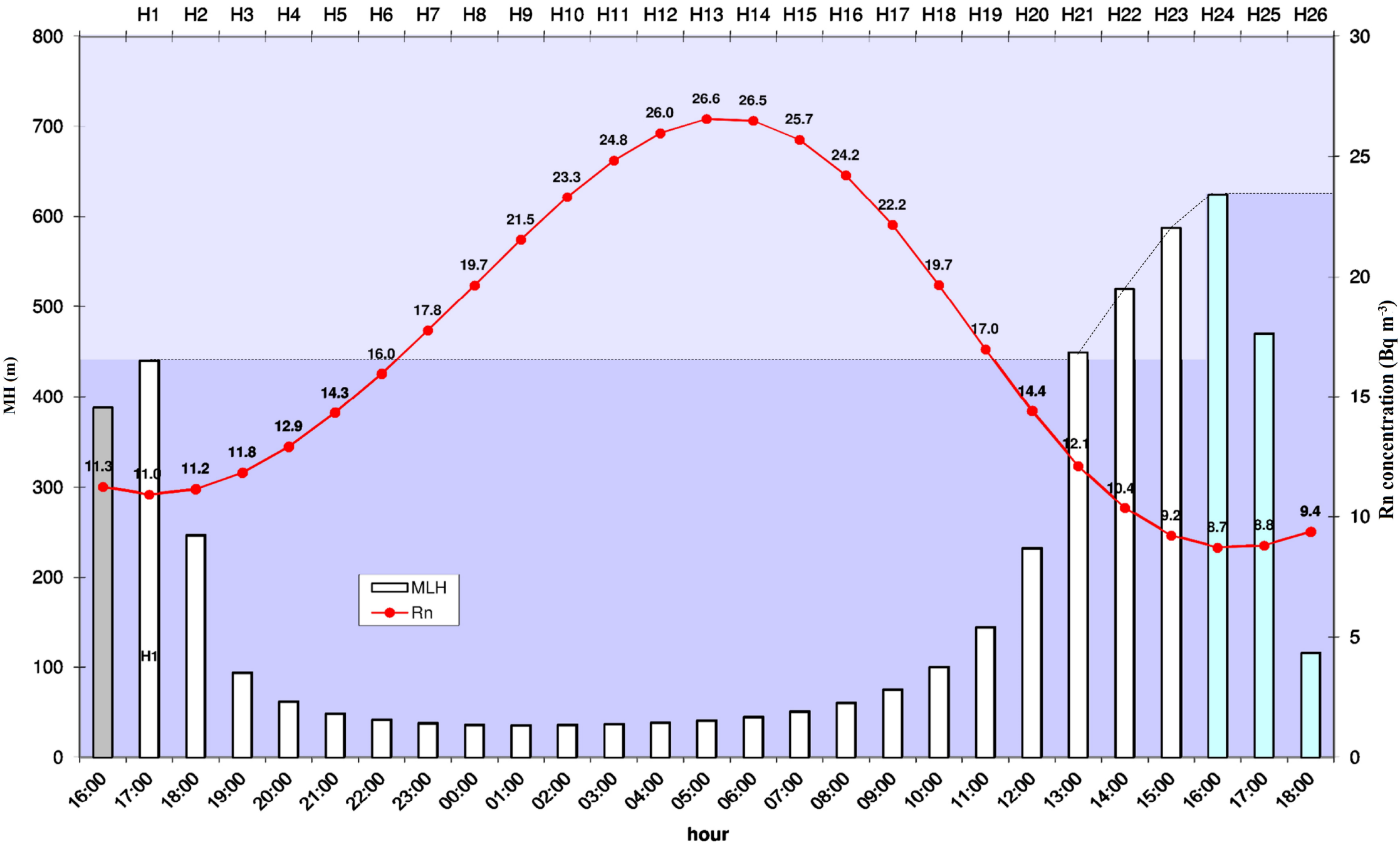
H1 H2 H3 H4 H5 H6 H7 H8 H9 H10 H11 H12 H13 H14 H15 H16 H17 H18 H19 H20 H21 H22 H23 H24 H25 H26
MH (m)
Rn concentration (Bq m-3)
MLH
Rn
11.3 11.0 11.2 11.8 12.9 14.3 16.0 17.8 19.7 21.5 23.3 24.8 26.0 26.6 26.5 25.7 24.2 22.2 19.7 17.0 14.4 12.1 10.4 9.2 8.7 8.8 9.4
H1
16:00 17:00 18:00 19:00 20:00 21:00 22:00 23:00 00:00 01:00 02:00 03:00 04:00 05:00 06:00 07:00 08:00 09:00 10:00 11:00 12:00 13:00 14:00 15:00 16:00 17:00 18:00
hour

Figure 5

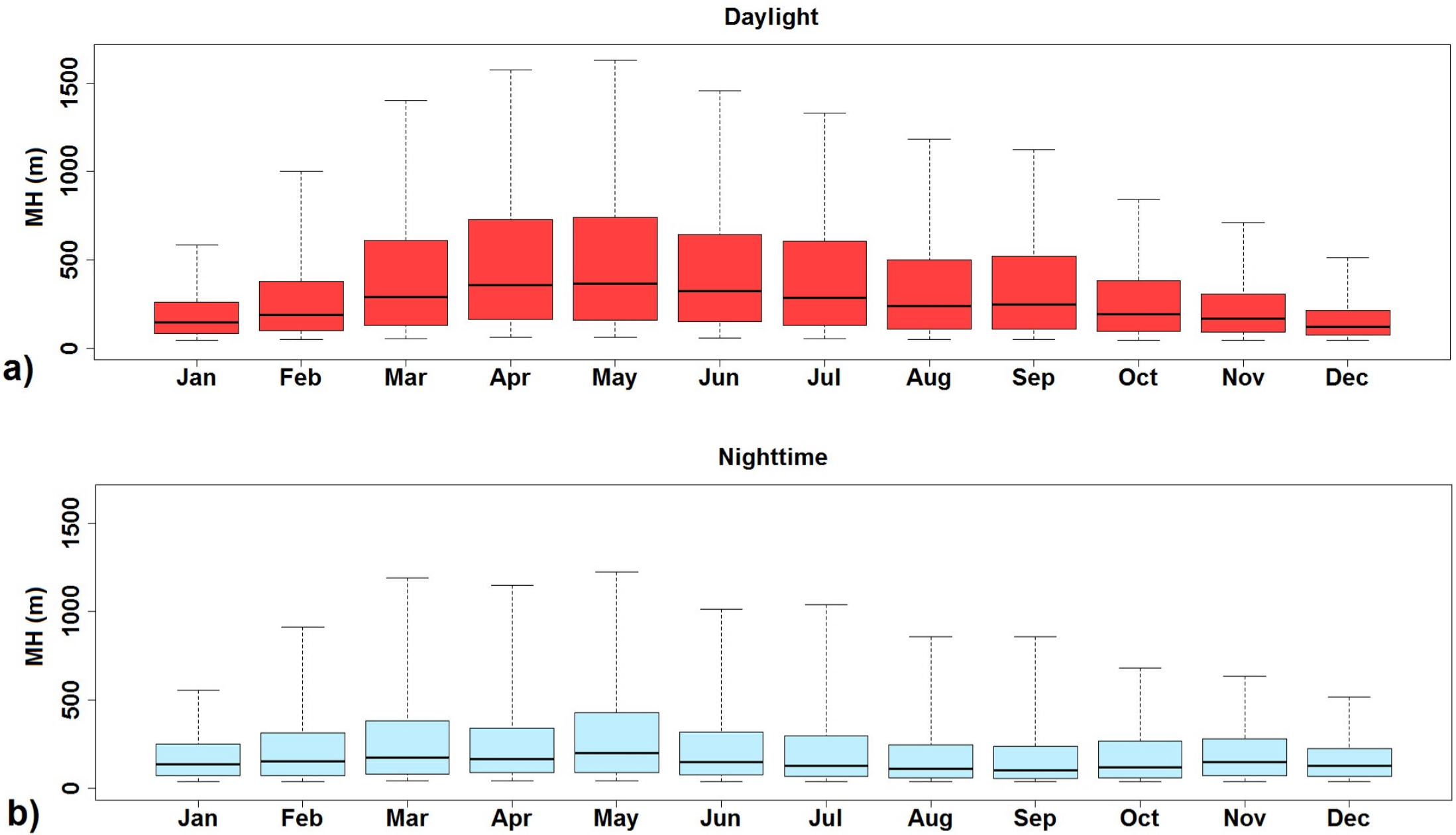
Daylight
MH (m)
0
500
1000
1500
Jan
Feb
Mar
Apr
May
Jun
Jul
Aug
Sep
Oct
Nov
Dec
a)
Nighttime
MH (m)
0
500
1000
1500
Jan
Feb
Mar
Apr
May
Jun
Jul
Aug
Sep
Oct
Nov
Dec
b)

Figure 6

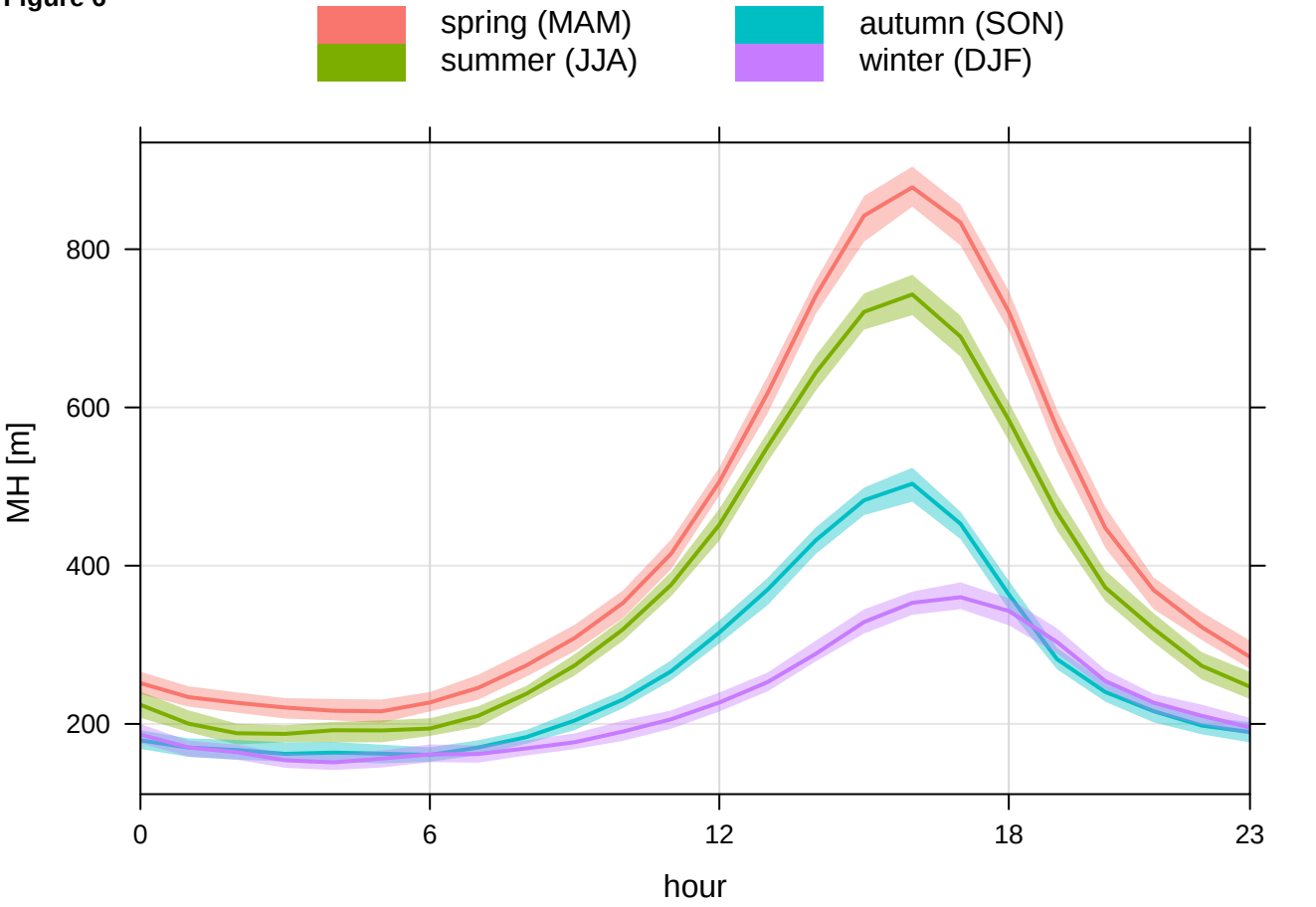
spring (MAM)
summer (JJA)
autumn (SON)
winter (DJF)
MH [m]
800
600
400
200
0
6
12
18
23
hour

Figure 7

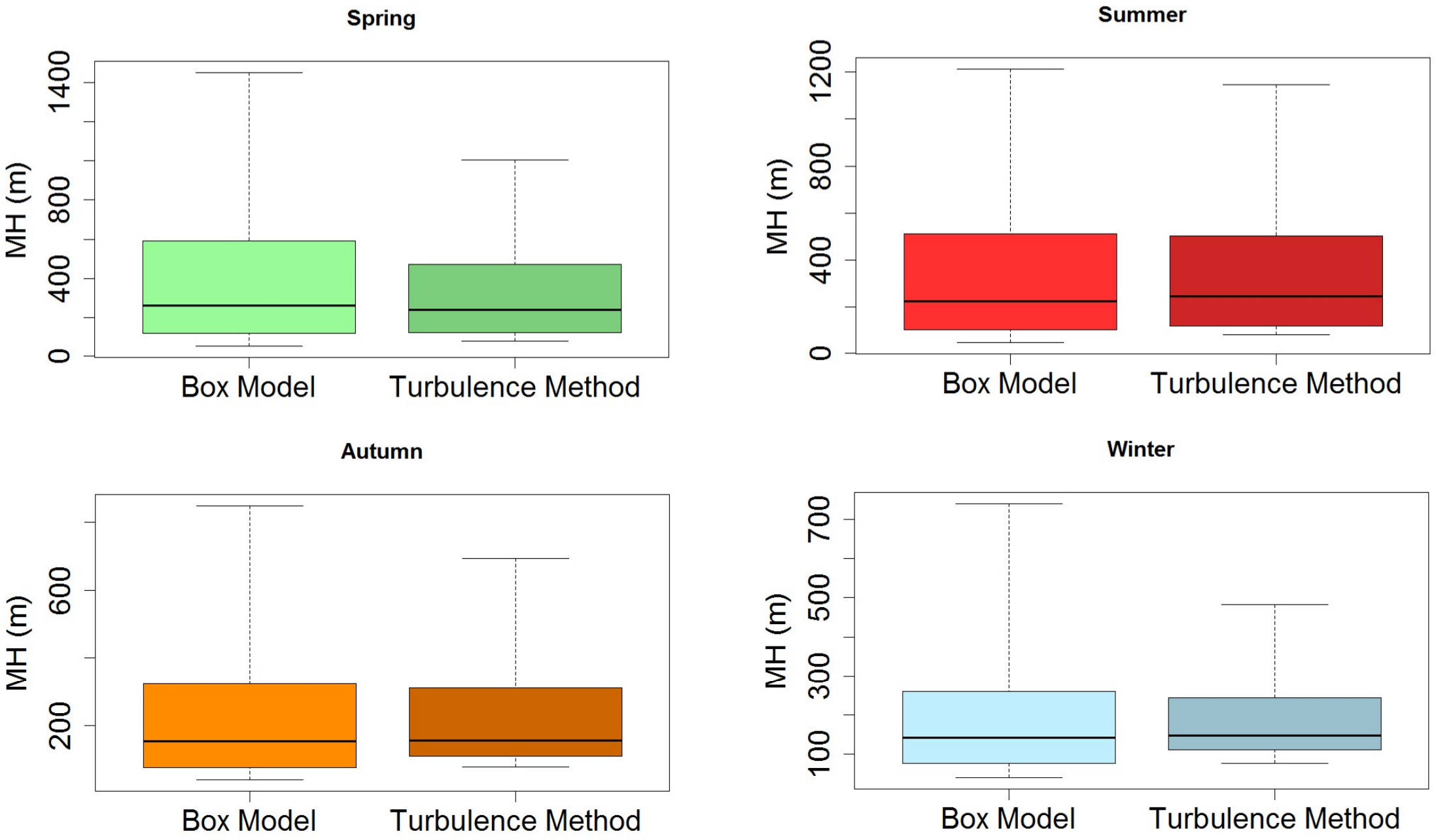
Spring
MH (m)
0
400
800
1400
Box Model
Turbulence Method
Summer
MH (m)
0
400
800
1200
Box Model
Turbulence Method
Autumn
MH (m)
200
600
Box Model
Turbulence Method
Winter
MH (m)
100
300
500
700
Box Model
Turbulence Method

Figure 8

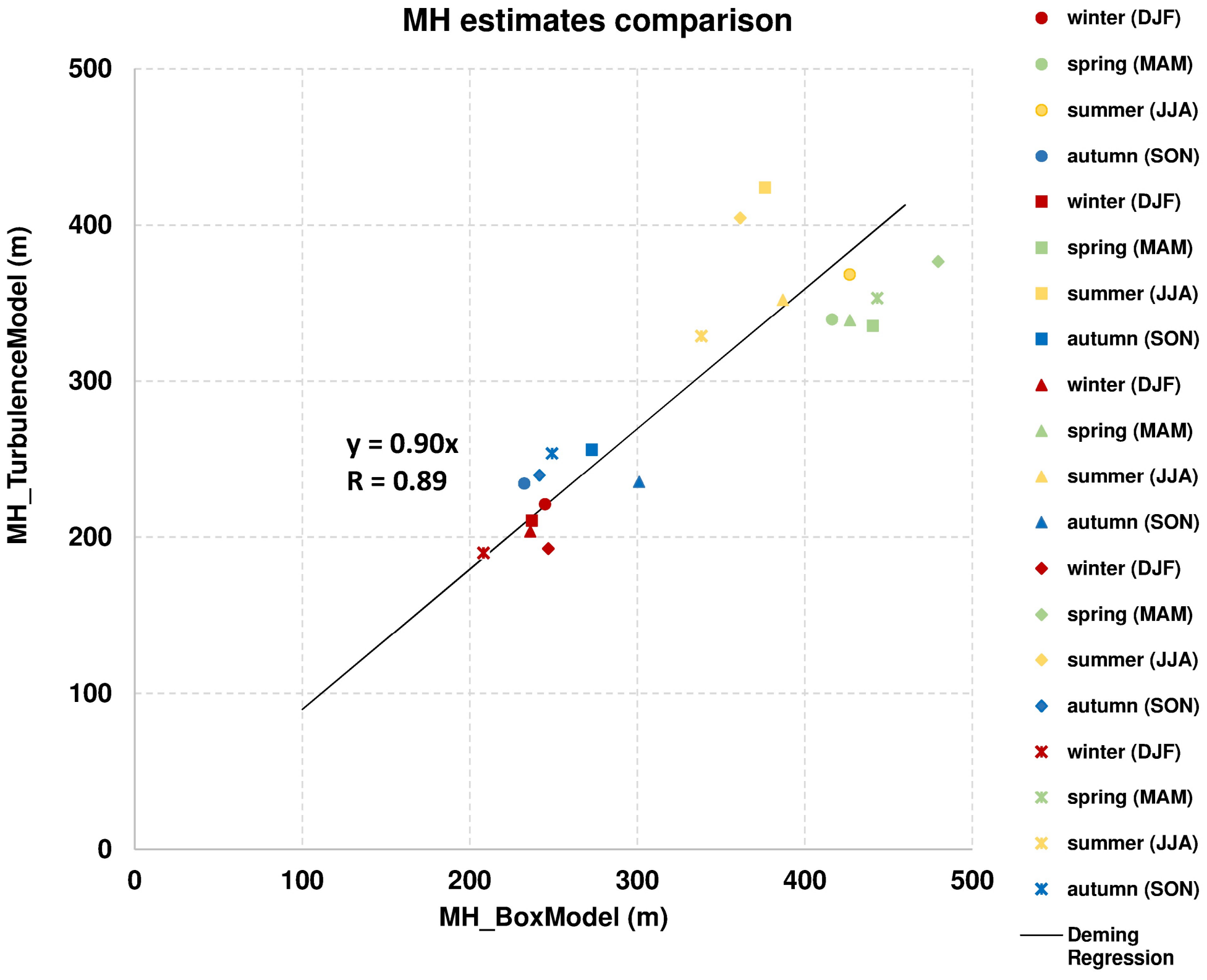
MH estimates comparison
MH_TurbulenceModel (m)
MH_BoxModel (m)
y = 0.90x
R = 0.89
0
100
200
300
400
500
winter (DJF)
spring (MAM)
summer (JJA)
autumn (SON)
Deming Regression

Supplementary Material

Click here to download Supplementary Material: Supplemental material_box-model_rev.pdf

Highlights

- Radon and its progeny are good markers for atmospheric dispersion conditions
- Short-lived radon decay products measured for 18 years with 30 min resolution
- A box model based on radon concentrations estimated equivalent mixing layer heights
- Radon-based and turbulence-based estimates for MH resulted comparable
- Radon measurements at monitoring stations could be effectively implemented

Graphical Abstract (for review)